CERN-NUFACT Note 051
November 8, 2000

Single Particle description of Ionization Cooling

G. Franchetti

Abstract

In this note we derive the stochastic equations which describe the single particle dynamics in an uniform cooling channel. Formulae and graphics for design optimizations are discussed.

1 Introduction

In future accelerator developments neutrino factories are an investigated issue [1]. Experimental requirements for neutrino physics and muons lifetime impose a set of constrains which are challenging for the design of the front-end linac after the target [2]. In order to meet design constrains, the large 6D beam emittance obtained after the target needs an effective fast cooling. Ionization cooling has been proposed as a method to cool transverse 4D emittance [2] while longitudinal cooling might be reached through a transverse-longitudinal emittance [3] exchange where the longitudinal emittance is transferred to the transverse plane and there cooled out. The main issue for an ionization cooling scheme become its effectiveness and optimization. In the international collaboration [4] efforts both theoretical [5, 6] and computational [7] have been dedicated to investigate beam dynamics in ionization cooling channels.

We report in this note a theoretical investigation based on a single particle dynamics. We present in some approximations the effects of absorber on the final value of the cooled emittance.

2 Modeling Ionization Cooling

Typically a cooling cell is built with focusing structures, absorbers,and cavities [8]. In this work we restrict the study at linear cooling cell (no bends). First we consider the dynamics in one plane. We consider the horizontal plane. In order to describe the single particle dynamics we introduce an orthogonal reference frame x, z. The transverse dynamical coordinates of one particle are $x, x' = dx/ds = p_x/p_z$. The cooling principle is the following [2]: the absorber reduces the particle's energy, but the cavity increases only the longitudinal momentum p_z. The global effect is a decreasing of x'. Next we describe the modeling of the cooling cell components.

2.1 Focusing Structures

In general if the focusing it is not to strong the particle's dynamics can be described by

$$x'' + kx = 0$$

where k is the focusing strength.

2.2 Absorbers

The motion of the particle through the absorber is affected by the muon-atom interaction which produces an absorption of energy ε and an angular deviation ψ from the incoming direction characterized by two distributions f_ε, f_ψ with standard deviations σ_ε and σ_ψ. The muon-atom interaction is repeated many times, say n, along the muon path through the absorber. The total energy absorption δE and angular deviation θ have standard deviations $\sigma_{\delta E} = \sqrt{n}\sigma_\varepsilon$ and $\sigma_\theta = \sqrt{n}\sigma_\psi$ and averages E_a, and $\tilde{\theta}$. If the number of interactions n for each particle is the same, i.e. if δE, and θ have small deviations from E_a, and $\tilde{\theta}$ we expect that the distributions of δE, and θ are are gaussian; for big deviations the number of interactions n is much bigger than for small $|\delta E - E_a|, |\theta - \tilde{\theta}|$ and the distributions present deviations from a gaussian tail [9]. Since for $|\theta| << 1$ we can write $\delta x' = \theta$, the absorber can

be modeled with the map

$$\begin{pmatrix} x \\ x' \\ E \end{pmatrix}_{out} = \begin{pmatrix} x + x' L_a + \delta x \\ x' + \delta x' \\ E - E_a + \delta E \end{pmatrix}$$

Here we consider $\delta x, \delta x', \delta E$ be gaussian random noises with standard deviations $\sigma_{\delta x}, \sigma_{\delta x'}, \sigma_{\delta E}$. L_a is the length of the absorber, and E_a is the average energy taken by the absorber when the average exit angle $\tilde{\theta}$ is x'. Note that the 3 random variables are decorrelated and that $\delta x'$ is not $(\delta x)'$.

2.3 Cavities

A cavity affects only the longitudinal momentum so that $p_z \to p_z + \Delta p_z$. The transport through the cavity is then approximated by

$$\begin{pmatrix} x \\ x' \\ E \end{pmatrix}_{out} = \begin{pmatrix} x \\ x'/(1 + \Delta p_z/p_z) \\ E + E_c \end{pmatrix}$$

E_c is the energy supplied by the cavity, according to the phase, and Δp_z is the longitudinal momentum lost and regained.

3 Single Particle Equation of Motion

If transverse focusing, absorber, and cavities have a 'weak' effect on the particle dynamics, then we can use a smooth approximation for the cooling. Here we suppose to spread uniformly along the cooling cell cavities and absorbers. We lose then the concept of cell, introducing the uniform cooling channel. An infinitesimal part of the channel of length ds can be approximated as a composition absorber + cavity + focusing kick plus a drift. The absorber-cavity-focusing kick is

$$\begin{pmatrix} x \\ x' \\ E \end{pmatrix}_{out} = \begin{pmatrix} x + \delta x \\ x' - x' \Delta p_z/p_z - k\, ds x + \delta x' \\ E + E_c - E_a + \delta E \end{pmatrix}$$

The drift map is

$$\begin{pmatrix} x \\ x' \\ E \end{pmatrix}_{out} = \begin{pmatrix} x + x'\,ds \\ x' \\ E \end{pmatrix}$$

Composing the transport map with the kick we obtain the map of the microcell

$$\begin{pmatrix} x \\ x' \\ E \end{pmatrix}_{out} = \begin{pmatrix} x + x'ds + \delta x + o(1) \\ x' - x'\Delta p_z/p_z - k\,ds\,x + \delta x' \\ E + E_c - E_a + \delta E \end{pmatrix} \tag{1}$$

When we track a particle by using Eq. 1, at each application of the map one should create $\delta x, \delta x'$, and δE. We postpone the discussion on δE and consider $\delta x'$ be a gaussian noise which variance depends on the distance ds according to

$$\sigma^2(\delta x') = \alpha ds \tag{2}$$

where α is a constant typical of the absorber and the beam energy. Eq. 2 keeps the consistency with the composition of noise errors along the absorber. For muons we have [9]

$$\alpha = \frac{f}{X_0}\left(\frac{13.6MeV}{\beta cp}\right)^2 \quad [m^{-1}]$$

where f is the absorber filling factor of the real periodic cooling cell, X_0 is the radiation length of the absorber, $\beta = v/c$, and p the particle momentum. From the particle's propagation through the absorber it is straightforward from Eq. 2 to see that $\sigma(\delta x) = \sigma(\delta x')ds/\sqrt{3}$. By using the Eq. 2 we find

$$\sigma^2(\delta_x) = \frac{\alpha}{3}ds^3 \tag{3}$$

Note that for small ds the noise δ_x become much smaller than the noise in δ'_x. This suggests that on the continuum δ_x will have a negligible effect on the dynamics.

From the first two rows of Eq. 1 we find

$$\begin{aligned} \Delta x &= x'\,ds + \delta x + o(1) \\ \Delta x' &= -x'\Delta p_z/p_z - k\,ds\,x + \delta x' \end{aligned}$$

dividing by ds the previous equations become

$$\begin{pmatrix} \Delta x/ds \\ \Delta x'/ds \end{pmatrix} = \begin{pmatrix} 0 & 1 \\ -k & -(\Delta p_z/p_z)/ds \end{pmatrix} + \begin{pmatrix} \delta x/ds \\ \delta x'/ds \end{pmatrix} \tag{4}$$

In order to extend to the continuum this difference equation we guess a sequence of N errors $\delta x'_j, j = 1, ..., N$ correspondent to the N application of the map Eq. 1. Each of these errors is generated by the same source which is gaussian with variance Eq. 2. The second term in the rhs second row of Eq. 4 can be extended to the continuum with the interpolation $\xi_{x'}(s) = \delta x'_j/ds = \xi'_j/\sqrt{ds}$ if $jds < s < (j+1)ds$, where now ξ'_j is a random variable such that $< \xi'_j \xi'_j >= \alpha$. When $ds \to 0$, $\xi_{x'}(s)$ become the derivative of the Wiener stochastic process [10, 11] which has the formal property

$$< \xi_{x'}(s)\xi_{x'}(s') >= \alpha\delta(s - s')$$

The same argument can be repeated for $\delta x/ds$ the second term on the first row in the rhs of Eq. 4. The extension to the continuum is $\xi_x(s) = \delta x_j/ds = \xi_j\sqrt{ds}$ if $jds < s < (j+1)ds$, where now ξ_j is a random variable such that $< \xi_j \xi_j >= \alpha/3$. When $ds \to 0$, $\xi_x(s) \to 0$: the stochastic noise on the spatial coordinates can be neglected. On the limit of ds to zero, $\xi_x(s)$ converges formally to a function which has the property

$$< \xi_x(s)\xi_x(s') >= \frac{\alpha}{3} ds^2 \delta(s - s')$$

With these definitions we finally write the transverse stochastic equation of motion for a particle in a 'uniform' cooling channel.

$$\begin{pmatrix} x \\ x' \end{pmatrix}' = \begin{pmatrix} 0 & 1 \\ -k & -d \end{pmatrix} + \begin{pmatrix} \xi_x \\ \xi_{x'} \end{pmatrix} \tag{5}$$

The term $d = (\Delta p_z/p_z)/ds$ can be computed as follow: with the assumption of $|x'| << 1$ each time the particle passes through the cavity+absorber the longitudinal momentum lost and regained Δp_z is a constant quantity throughout the cooling channel. On the other hand energy conservation between the entrance and exit of the cavity leads to

$$\sqrt{p_{z,in}^2(1 + x_{in}'^2)c^2 + (mc^2)^2} + qV = \sqrt{p_{z,out}^2(1 + x_{out}'^2)c^2 + (mc^2)^2}$$

and here $x'_{out} = x'_{in}(1 - \Delta p_z/p_{z,out})$. Since qV is small with respect to the energy of the particle, an expansion at the first order gives

$$d = (\Delta p_z/p_z)/ds = \frac{V}{ds}\frac{q}{E_0\beta_z^2}$$

The average electric field (longitudinal RF density) V/ds depends form the energy taken by the absorber $E_a + \delta E$, in fact along each ds the RF voltage has to restore the lost momentum Δp_z and this happens when

$$\frac{E_a + \delta E}{1 + x'^2_{in}} = qV$$

that with smooth approximations become $E_a + \delta E = qV$. Since $\sigma^2_{\delta E} \propto ds$ and $E_a \propto ds$ we find that $\sigma_{\delta E}/E_a \propto 1/\sqrt{ds}$. In order to simplify the problem we assume here that ds is such that $\sigma_{\delta E}/E_a << 1$ so that we can neglect the energy fluctuation δE and assume $E_a = qV$. For a cooling cell of length L the coefficient d can be approximated as

$$d = \frac{\Delta E}{E_0}\frac{1}{L\beta_z^2}$$

where ΔE is the energy lost and gained per cell.

A generalization of Eq. 5 at the 2D case is given by the set of equations

$$\mathbf{X}' + M\mathbf{X} = \mathbf{N} \tag{6}$$

with

$$\mathbf{X} = \begin{pmatrix} x \\ x' \\ y \\ y' \end{pmatrix} \quad \mathbf{N} = \begin{pmatrix} \xi_x \\ \xi_{x'} \\ \xi_y \\ \xi_{y'} \end{pmatrix} \quad M = \begin{pmatrix} 0 & -1 & 0 & 0 \\ k_q & d & \hat{k}_q & -k_s \\ 0 & 0 & 0 & -1 \\ \hat{k}_q & k_s & k_q & d \end{pmatrix} \tag{7}$$

This equations includes the constant focusing uniform channel modeled by Eq. 5 included with the coefficient k_q; it includes the uniform solenoidal cooling channel, by the coefficient k_s

$$\mathbf{x}'' = \mathbf{x}' \wedge \mathbf{s}k_s + d\mathbf{x}' \tag{8}$$

with $\mathbf{s}$ longitudinal versor and $k_s = qB_0/p_z$; or more general combinations of uniform focusing, uniform solenoid, and uniform skew quadrupole (the coefficient $\hat{k}_q$) in the cooling channel. Next we show the method to solve Eq. 6

4 Single Particle Dynamics

The simplest case would be a cooling channel with quadrupoles which keeps both transverse planes decoupled. However it has been proposed a more efficient scheme [12] which uses alternating solenoids. For an axially symmetric beam in a solenoidal channel, envelope equations have been derived by R. K. Cooper [13], and recent works had included the effect of the absorbers [5, 6]. In the next discussion we calculate the effect of the noise on the single particle dynamics in a uniform channel where the cooling channel properties are constant along the longitudinal direction.

We first solve Eq. 6 considering $\mathbf{N}$ as a well defined function. Consider the transformation $\mathbf{Z} = P^{-1}\mathbf{X}$ where P is the invertible matrix which diagonalize M. Eq. 6 become

$$\mathbf{Z}' = \Lambda\mathbf{Z} + P^{-1}\mathbf{N} \tag{9}$$

with $\Lambda = P^{-1}MP = diag(\lambda_1, \lambda_2, \lambda_3, \lambda_4)$ and λ_i eigenvalues of the matrix M. Eq. 9 is a set of decoupled first order differential equation of the form

$$z_i' = \lambda_i z_i + \sum_j (P^{-1})_{ij}\mathbf{N}_j \quad i = 1, 2, 3, 4 \tag{10}$$

The solution for the i component is

$$z_i(s) = \sum_j C_{ij}e^{\lambda_j s} + e^{\lambda_i s}\int_0^s e^{-\lambda_i s'}\sum_j (P^{-1})_{ij}\mathbf{N}_j(s')ds' \tag{11}$$

where C_{ij} is a matrix determined by the initial conditions. Returning back to the original variables we find

$$x_k(s) = \sum_{ij} P_{ki}C_{ij}e^{\lambda_j s} + \sum_{ij} P_{ki}e^{\lambda_i s}\int_0^s e^{-\lambda_i s'}(P^{-1})_{ij}\mathbf{N}_j(s')ds' \tag{12}$$

The first term on the rhs represents the homogeneous solution of Eq. 6 that we call $\hat{x}_k(s)$ while the second term represents the contribution of $\mathbf{N}$ here called Δx_k. The evolution of $\Delta x_k(s)$ depends on the noise $\mathbf{N}(s)$ which is a function that has a certain probability to be found in the set of all the possible choices for $\mathbf{N}$. We indicate this dependence changing the notation and calling the contribution of the noise with $\Delta x_k[\mathbf{N}]$ meaning that, only if we fix the

function noise $\mathbf{N}$ then $\Delta x_k[\mathbf{N}]$ can be computed. In this sense we cannot characterize the dynamics of a single particle with a unique solution, but rather we can give a probability $\mathcal{P}[\mathbf{N}]d[\mathbf{N}]$ that the noise has the functional form $\mathbf{N}(s)$ and then compute the motion. It follows then naturally that the frame for a predictive analytical investigation must be statistical. At the longitudinal position s each coordinate of the particle has the value $x_k(s) = \hat{x}_k(s) + \Delta x_k[\mathbf{N}](s)$ with probability $\mathcal{P}[\mathbf{N}]d[\mathbf{N}]$. We can average with respect to the noise and find

$$\langle x_k \rangle_{\mathbf{N}}(s) = \hat{x}_k(s) + \langle \Delta x_k[\mathbf{N}] \rangle_{\mathbf{N}}(s)$$

where here with $\langle \cdot \rangle_{\mathbf{N}}$ we mean average over the noise. Since the noise $\mathbf{N}$ has average zero we find $\langle x_k \rangle_{\mathbf{N}}(s) = \hat{x}_k(s)$. We can also characterize the spread of $x_k(s)$ computing the variance

$$\langle (x_k(s) - \hat{x}_k(s))^2 \rangle_{\mathbf{N}} = \langle \Delta x_k^2[\mathbf{N}] \rangle_{\mathbf{N}}(s)$$

However for an rms approach to the beam description, moments like $\overline{xx'}$ are needed requiring the evaluation of all the noise correlations (See Appendix B). We call to simplify the notations $\Delta_{kp}(s) = \langle \Delta x_k[\mathbf{N}] \Delta x_p[\mathbf{N}] \rangle_{\mathbf{N}}(s)$. By using the second term on the rhs of Eq. 12 we find

$$\Delta_{kp}(s) =$$

$$= \sum_{ijqt} P_{ki} (P^{-1})_{ij} P_{pq} (P^{-1})_{qt} \int_0^s \int_0^s e^{-\lambda_i(s'-s) - \lambda_q(s''-s)} \langle \mathbf{N}_j(s') \mathbf{N}_t(s'') \rangle_{\mathbf{N}} ds' ds'' \tag{13}$$

However

$$\langle \mathbf{N}_j(s') \mathbf{N}_t(s'') \rangle_{\mathbf{N}} = \int_{\mathcal{F}} \mathbf{N}_j(s') \mathbf{N}_t(s'') \mathcal{P}[\mathbf{N}] d[\mathbf{N}] = Q_{jt} \delta(s' - s'') \tag{14}$$

with $\mathcal{F}$ is the space of the noises and $\delta(s' - s'')$ is Dirac's function. The matrix Q_{jt} has the form

$$Q = \begin{pmatrix} \alpha ds^2/3 & 0 & 0 & 0 \\ 0 & \alpha & 0 & 0 \\ 0 & 0 & \alpha ds^2/3 & 0 \\ 0 & 0 & 0 & \alpha \end{pmatrix} \tag{15}$$

where ds is the integration length used in Eq. 1. The diagonal form of Q stems from the decorrelation of the noises in the four coordinates. The second order terms in ds give second order terms in ds on the final expression of $\Delta_{kp}(s)$. Since we are considering very small integration step we can drop the second order terms in Eq. 15 neglecting then the noises ξ_x, ξ_y. With this approximation and defining the matrix

$$L = \begin{pmatrix} 0 & 0 & 0 & 0 \\ 0 & 1 & 0 & 0 \\ 0 & 0 & 0 & 0 \\ 0 & 0 & 0 & 1 \end{pmatrix}$$

Eq. 13 gets the form

$$\Delta_{kp}(s) = \alpha \sum_{ijqt} P_{ki}(P^{-1})_{ij} P_{pq}(P^{-1})_{qt} L_{jt} \frac{1 - e^{(\lambda_i + \lambda_q)s}}{-(\lambda_i + \lambda_q)} \tag{16}$$

Defining the symmetric matrix $B = P^{-1} L P^{-1T}$ and

$$F_{iq}(s) = \frac{1 - e^{(\lambda_i + \lambda_q)s}}{-(\lambda_i + \lambda_q)} \tag{17}$$

we can express the noise correlations in the compact form

$$\Delta_{kp}(s) = \alpha \sum_{iq} P_{ki} P_{pq} B_{iq} F_{iq}(s) \tag{18}$$

From this expression we see that a crucial role is played by the sum $\lambda_i + \lambda_q$: if this sum has real part negative the function F_{iq} approaches an asymptotic value for big s, if $Re(\lambda_i + \lambda_q) > 0$ the effect of the noise increases exponentially; if $Re(\lambda_i + \lambda_q) = 0$ then $F_{iq} = s$.

5 Uniform Quadrupolar Cooling Channel

In a quadrupolar uniform cooling channel horizontal and vertical planes are decoupled and the matrix M of Eq. 6 gets the blocks diagonal form

$$M = \begin{pmatrix} 0 & 1 \\ -k & -d \end{pmatrix} \otimes \begin{pmatrix} 0 & 1 \\ -k & -d \end{pmatrix}$$

We consider then only the horizontal plane. The general solution of the equation

$$x'' + dx' + kx = n_{x'} \tag{19}$$

is

$$x = Ae^{\lambda_1 s} + Be^{\lambda_2 s} - \frac{e^{\lambda_1 s}}{\lambda_2 - \lambda_1} \int_0^s n_{x'}\, e^{-\lambda_1 s'} ds' + \frac{e^{\lambda_2 s}}{\lambda_2 - \lambda_1} \int_0^s n_{x'}\, e^{-\lambda_2 s'} ds' \tag{20}$$

where λ_1, λ_2 are the eigenvalues $\lambda_1 = -d/2 + \sqrt{d^2 - 4k}$ and $\lambda_2 = -d/2 - \sqrt{d^2 - 4k}$. Eq. 20 is just Eq. 8 for $k = 1$ and it is valid if $d^2 \neq 4k$. First we study the solution when the absorber noise is absent.

5.1 Unperturbed Solution $n_{x'} = 0$

In this case the solution become

$$x = e^{-d/2s}[Ae^{\sqrt{d^2-4k}s} + Be^{-\sqrt{d^2-4k}s}]$$

the factor $e^{-d/2s}$ is the exponential damping of the particle motion, while the terms inside the square brackets depends on $\sqrt{d^2 - 4k}$. We can distinguish two regimes, one where the focusing strength dominates the damping i.e. when $\sqrt{d^2 - 4k}$ is pure complex and the terms in the square brackets express an oscillation. The other regime is dominated by the damping over the focusing strength, in this case $\sqrt{d^2 - 4k}$ is real.

5.1.1 Focusing Dominated Regime

In the focusing dominated regime $d^2 < 4k$ and calling $\sqrt{4k - d^2} = K$ the solution in terms of the initial condition becomes

$$x = e^{-d/2s} \left[x_0 \left(-\frac{d \sin(K/2s)}{K} + \cos(K/2s) \right) + \frac{2x_0'}{K} \sin(K/2s) \right] \tag{21}$$

The dissipative term dx' in Eq. 19 causes a dumping of energy $E = x'^2/2 + kx^2/2$ according to $E' = -dx'^2$. However in the quadrupolar channel the particle energy changes continuously form between potential energy and kinetic

energy. If the change of E is not to fast compared with the period of one betatron oscillation an equipartition argument leads to the relation $E = \langle x'^2 \rangle$ (over one betatron oscillation). We find then the equation $E' = -dE$ which shows to a dump of the energy with the factor $\exp(-d\,s)$.

We observe that if $d \to 0$ then $K/2 \to \sqrt{k}$ and the previous solution approaches the usual

$$x = x_0 \cos(\sqrt{k}s) + \frac{x_0'}{\sqrt{k}} \sin(\sqrt{k}s)$$

which express the betatronic motion in a uniform focusing channel. When $d > 0$ the oscillation are damped according to $e^{-d/2s}$. If we are in a regime where $k >> d$ the term $d\sin(K/2s)/K$ become smaller than $\cos(K/2s)$ and the exact solution can be approximated by

$$x = e^{-d/2s}[x_0 \cos(\sqrt{k}s) + \frac{x_0'}{\sqrt{k}} \sin(\sqrt{k}s)] \tag{22}$$

5.1.2 Envelope and Emittance Evolution

Since the focusing strength is uniform the twiss parameters of the cooling channel are $\beta = 1/\sqrt{k}, \gamma = 1/\beta$ and the initial coordinates x_0, x_0' can be expressed as

$$x_0 = \sqrt{\beta\epsilon_0}\sin\hat{\delta} \qquad x_0' = \sqrt{\gamma\epsilon_0}\cos\hat{\delta}$$

with $\hat{\delta}$ an initial phase. By using these expressions in Eq. 22 we find

$$x = e^{-d/2s}\sqrt{\beta\epsilon_0}\sin(\sqrt{k}s + \hat{\delta}) \tag{23}$$

consequently the single particle emittance evolves according to

$$\epsilon_x(s) = \epsilon_{x,0}e^{-ds}$$

The same relation holds for the matched beam and the envelope $\hat{x}_{env}$ evolves according to $\hat{x}_{env} = \hat{x}_{env,0}\exp(-d/2s)$. When we approach the transition condition $4k = d^2$ Eq. 23 does not hold since the oscillation term $d\sin(K/2s)/K$ in Eq. 21 is not negligible. However the solution Eq. 21 holds and can be used giving a solution like

$$x = e^{-d/2s}[oscillating \quad terms] \qquad x' = e^{-d/2s}[oscillating \quad terms]$$

Again by using $\epsilon_x = \beta x'^2 + \gamma x^2$ one finds that

$$\epsilon_x(s) = e^{-ds}[oscillating \quad terms]$$

which shows the exponential damping of the single particle emittance.

5.1.3 Damping Dominated Regime

This regime happens when $4k < d^2$. Defining $\sqrt{d^2 - 4k} = K$ the solution of the motion become

$$x = \frac{2}{K}[(x_0(K + d/2) + x_0')e^{-d/2s+Ks} + (x_0(K - d/2) - x_0')e^{-d/2s-Ks}]$$

Since $-d/2 \pm K < 0$ the motion is dumped and no betatron motion can be found. The transverse kinetic energy is not converted in potential but rather taken by the absorber.

5.2 Noise Effect

Applying the theory described in Section 4 to the uniform quadrupole channel for $d^2 \neq 4k$ we find

$$\Delta_{11} = \Delta_{33} = \frac{\alpha}{d^2 - 4k}\left\{\frac{1}{2k}[d - e^{-ds}(d\cosh(\xi s) + \xi \sinh(\xi s))] - \frac{2}{d}(1 - e^{-ds})\right\} \tag{24}$$

$$\Delta_{22} = \Delta_{44} = \frac{\alpha}{d^2 - 4k}\left\{\frac{1}{2}[d + e^{-ds}(-d\cosh(\xi s) + \xi \sinh(\xi s))] - \frac{2k}{d}(1 - e^{-ds})\right\}$$

and

$$\Delta_{12} = \Delta_{34} = \frac{\alpha}{d^2 - 4k}\left\{e^{-ds}(\cosh(\xi s) - 1)\right\}$$

with $\xi = \sqrt{d^2 - 4k} = K$ in the dumping dominated regime ($d^2 > 4k$) and $\xi = -i\sqrt{4k - d^2} = -iK$ in the focusing dominated regime ($d^2 < 4k$). All the missing moments are zero.

We can visualize how the noise disturbs the particle dynamics integrating the equations of motion Eq. 1. We have considered as example a uniform quadrupolar cooling channel with parameters $k = 1$ m^{-2}, $d = 0.1$ m^{-1}, $\alpha = 5.9 \cdot 10^{-4}$ rad^2/m. Given a particle with initial coordinates $x = 0.3$

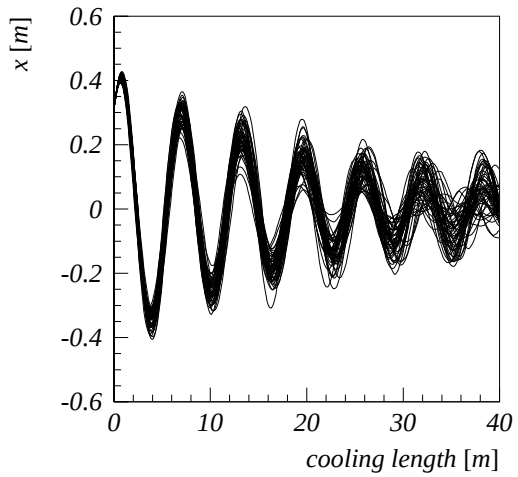

Figure 1: Example with 50 repetition of a particle's trajectory: each time the absorber noise build up an error in a different way.

m, $x' = 0.3$ rad, in order to show the stochastic nature of the motion, we repeated the integration 50 times. Fig. 1 shows this result. Note that the spread of the curves at each longitudinal position s increases with s showing the effect of the noise on the dynamics. The picture shows that when the spread of the particle equals the betatron amplitude the cooling stop to be effective. From the numerical integration (Fig. 1), at each s we can compute the standard deviation of the particle's position and compare it with the prediction of the theory i.e. $\sqrt{\Delta_{11}}$. This is shown in Fig. 2: the agreement is very good. Next we include the noise effect on the particle dynamics in a focusing dominated regime.

5.2.1 Envelope with Noise in a Focusing Dominated Regime

The maximum spread Δx of one particle's position can be in principle big, but with very low probability. For practical considerations the maximum Δx is $\Delta x_{max} = 3\sqrt{\Delta_{11}}$. The envelope can be computed as the unperturbed envelope $\hat{x}_{env}$ plus Δx_{max} i.e.

$$x_{env}(s) = \hat{x}_{env}(s) + 3\sqrt{\Delta_{11}}$$

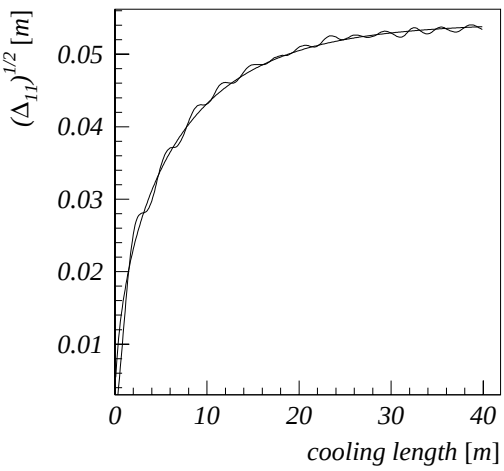

Figure 2: Comparison between the theoretical standard deviation and that one obtained from simulations by repeating the integration of the equation of motion with noise 10000 times.

substituting the expressions of $\hat{x}_{env}$, Δ_{11}, and neglecting small oscillating terms we find

$$x_{env}(s) = \sqrt{\beta\epsilon_0}e^{-d/2s} + 3\sqrt{\frac{\alpha}{2kd}(1 - e^{-ds})} \tag{25}$$

This equation can be rewritten in normalized units dividing by $\hat{x}_{env}(0)$. Defining $R = x_{env}(s)/x_{env}(0)$ we find

$$R = e^{-d/2s} + \frac{1}{\chi}\sqrt{1 - e^{-ds}}$$

where $\chi = (\sqrt{\beta\epsilon_0}/3)\sqrt{2kd/\alpha}$ is a dimensionless characteristic parameter which combines beam parameters and cooling channel parameters. Note that $R(0) = 1$ and $R(\infty) = 1/\chi$ and that R reaches a maximum $R = \sqrt{1 + 1/\chi^2}$ in $d\,s = -\ln(\chi^2/(1 + \chi^2))$.

A numerical check of Eq. 25 was performed. Fig. 3 shows the dumped oscillating motion of one particle, in red the theoretical dump of the envelope when the absorber noise is absent. The blue curve is the maximum contribution of the noise (3 times the standard deviation of the absorber noise),

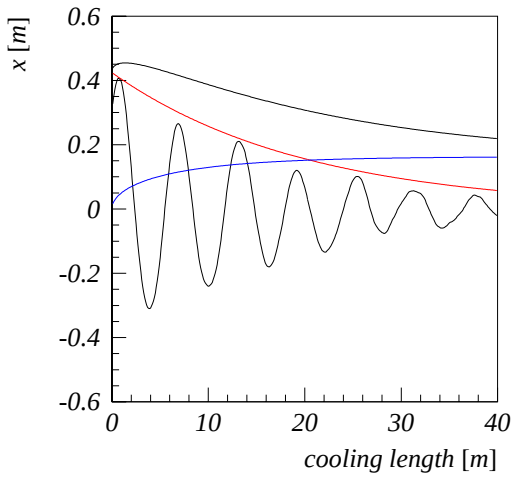

Figure 3: Example of one particle's trajectory when perturbed by the absorber noise. In red and blue the theoretical envelope and the noise error respectively. On the top in black the sum of the two curves.

while the black upper continuous curve represents the sum of the two curves (Eq. 25). The figure shows how the noise perturbs the dumped betatronic motion and that the theoretical prediction bounds this motion. In Fig. 4 is shown that the theoretical envelope really bound most of the possible trajectory that the absorber noise may build. Following the same argument used to compute x_{env} it is possible to obtain an analytical expression for x'_{env}. These two expression have the interesting property $x_{env}/\sqrt{\beta} = x'_{env}/\sqrt{\gamma}$ which is consistent with a new emittance that includes the effect of the noise and that can be expressed as $\epsilon_x = \epsilon_{x,0} R^2$. We conclude this section observing that the maximum cooling is reached for an infinitely long cooling channel. Practical considerations must be included in the discussion for a proper compromise between cooling performance and costs.

6 Uniform Solenoidal Cooling Channel

The main characteristic of particle's dynamics in a uniform solenoid is that a particle in this field would move on an helicoidal trajectory around an

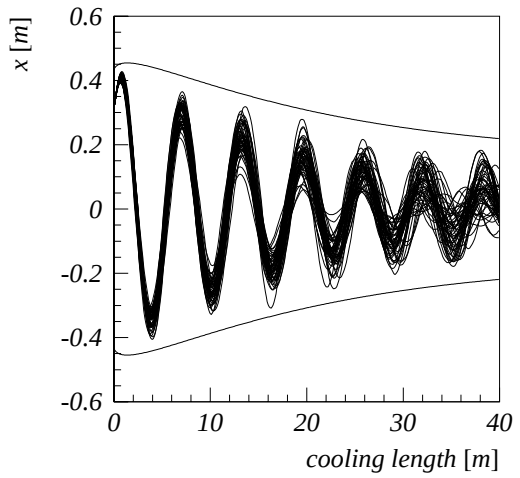

Figure 4: Comparison of the theoretical envelope with a set of 50 curves. The picture shows that the theoretical prediction bound practically all the trajectory evolution.

axis determined by the initial condition of the particle. In our theoretical description we assumed a particular frame for the uniform cooling channel: for the quadrupolar cooling channel the transverse origin is placed in the transverse center where the focusing force is zero. However in the case of a uniform solenoid this reference frame it is not privileged with respect to another transversally shifted because the uniform solenoid focuses the particle locally. The uniformly distributed absorber exhibits the same feature, i.e. its effect on the dynamics is invariant over transverse translations. For the uniform solenoidal cooling channel the system of equations of motion (in this global frame) have the form

$$\begin{cases} x'' = ky' - dx' + n_x \\ y'' = -kx' - dy' + n_y \end{cases} \tag{26}$$

where $k = qB_0/p_z$ and $d = (\Delta E/E_0)/(\beta_z^2 L)$. Here B_0 is positive if the vector magnetic field is parallel to the versor $\hat{z}$. When the noise is absent this

equations can be integrated and give the solution

$$\begin{cases} \hat{x}(s) = x_c - e^{-ds} R_0 \cos(ks - \theta) \\ \hat{y}(s) = y_c + e^{-ds} R_0 \sin(ks - \theta) \end{cases} \tag{27}$$

where $x_c = x_0 + (x_0' d + y_0' k)/(d^2 + k^2)$, $y_c = y_0 + (-x_0' k + y_0' d)/(d^2 + k^2)$ are the coordinates of the guide ray where the particle stops when the transverse motion is completely dumped. $R_0 = \sqrt{(x_0'^2 + y_0'^2)/(k^2 + d^2)}$ is the initial distance of the particle form x_c, y_c, and the initial phase θ is obtained by the equations $\cos\theta = (x_c - x_0)/R_0$, and $\sin\theta = (y_c - y_0)/R_0$.

Eq. 27 shows, as previously discussed, that all the particles with the same normalized transverse kinetic energy $E_{k0} = (x_0'^2 + y_0'^2)/2$ evolve in the same way with respect to their own guide ray, less an initial phase θ. Let's consider then a particle matched in the global reference frame, i.e. such that $x_c = y_c = 0$. The particle's motion described by Eq. 27 show a dumping in a characteristic length of $1/d$ which is twice the characteristic dump length for the uniform quadrupolar cooling channel. This stems from the lack of potential energy in this system: during its path the particle has only kinetic energy which gets absorbed continuously while for the quadrupolar channel only half of the energy (in average) is in kinetic form. From the point of view of the cooling process it is important to describe the evolution of $R = \sqrt{(x - x_c)^2 + (y - y_c)^2}$, and $E_k = (x'^2 + y'^2)/2$. By using Eq. 27 it is straightforward to show that for a matched particle (i.e. for every particle)

$$\hat{R} = R_0 e^{-ds} \tag{28}$$

and

$$\hat{E}_k = E_{k0} e^{-2ds}$$

The relation between $\hat{E}_k$ and $\hat{R}$ is

$$\hat{E}_k = \frac{d^2 + k^2}{2} \hat{R}^2$$

Here we use the symbol $\hat{\cdot}$ for the quantities computed without noise.

6.1 Noise Effect in a Solenoidal Uniform Channel

During the cooling process the absorber produces a noise which disturbs the dynamics. This effect is expected to be strong when the transverse kinetic

energy is comparable with the kinetic energy fluctuations induced by the absorber. In this condition the existence of infinitum stable orbits in a uniform solenoidal field allows the particle to move in any transverse position. In fact the absorber kick changes randomly the center of rotation (guide ray) of the particle along the channel. We expect that once the transverse kinetic equilibrium has been reached, a slow diffusive process will increase the particle's transverse position letting unchanged the average transverse kinetic energy. In this section we compute the evolution of the noise following the general theory presented in Section 4. The matrix M associated to system of the differential equations Eq. 26 is

$$M = \begin{pmatrix} 0 & 1 & 0 & 0 \\ 0 & -d & 0 & k \\ 0 & 0 & 0 & 1 \\ 0 & -k & 0 & -d \end{pmatrix}$$

It is straightforward to find that for this matrix the eigenvalues are

$$\lambda_1 = \lambda_2 = 0, \quad \lambda_3 = -d - ik, \quad \lambda_4 = -d + ik \tag{29}$$

the matrix P is

$$P = \begin{pmatrix} 0 & 1 & -i/(d+ik) & i/(d-ik) \\ 0 & 0 & i & -i \\ 1 & 0 & -1/(d+ik) & -1/(d-ik) \\ 0 & 0 & 1 & -1 \end{pmatrix} \tag{30}$$

and its determinant is $2i \neq 0$. Therefore P is invertible for all k, and d (when $k = 0$ the matrix P become real). Applying

$$\Delta_{kp}(s) = \alpha \sum_{iq} P_{ki} P_{pq} B_{iq} F_{iq}(s)$$

obtained in Section 4 we find

$$\begin{aligned}
&\Delta_{11} = \Delta_{33} = \alpha \left\{ \tfrac{1-e^{-2ds}}{2d(d^2+k^2)} - \tfrac{2e^{-ds}(de^{ds} - d\cos(ks) + k\sin(ks))}{(k^2+d^2)^2} + \tfrac{s}{d^2+k^2} \right\} \\
&\Delta_{12} = \Delta_{34} = \tfrac{\alpha}{2(d^2+k^2)} \left\{ 1 + e^{-2ds} - 2e^{-ds}\cos(ks) \right\} \\
&\Delta_{13} = \Delta_{24} = 0 \\
&\Delta_{14} = -\Delta_{23} = \tfrac{\alpha}{2d(d^2+k^2)} \left\{ k(-1 + e^{-2ds}) + 2de^{-ds}\sin(ks) \right\} \\
&\Delta_{22} = \Delta_{44} = \tfrac{\alpha}{2d}(1 - e^{-2ds})
\end{aligned} \tag{31}$$

All the moments can be found from Eqs. 31 by using the relations $\Delta_{ij} = \Delta_{ji}$. Note the term $s/(d^2 + k^2)$ in Δ_{11} and Δ_{33} which expresses the limitless diffusive motion due to the random noise. The linear dependence of s is consistent with the gaussian composition of the standard deviations. In fact when the absorber noise start to change the particle's transverse position, the motion of the particle become like a random walk. The composition of many absorber spatial kicks $\delta x, \delta y$ in a certain path along the channel creates the shifts $\Delta x, \Delta y$ which have a gaussian distribution. Moving along the channel the particle receives a number of transverse kicks which is proportional to the length s and the variance of the gaussian distribution of Δx, and Δy must be proportional to s. For practical application were $d << 1$ in the moments Δ_{11}, Δ_{33} we can drop the second term and get the simplified form

$$\Delta_{11} = \Delta_{33} = \frac{\alpha}{k^2 + d^2} \left\{ \frac{1}{2d}(1 - e^{-2ds}) + s \right\} \tag{32}$$

Similar tests on the terms Δ_{ij} as made for the quadrupolar channel were performed for the uniform solenoidal cooling channel. We started repeating 10 times the same simulation for a particle with initial condition $x = y = 0$ m, $x' = 1$ rad, $y' = -1$ rad. The parameter of the channel are: length = 150 m, $k = 0.5$ m^{-1}, $d = 0.1$ m^{-1}, $\alpha = 10^{-2}$ rad^2/m. Fig. 5 shows the diffusion after the transverse kinetic energy has reached the minimum. Fig. 6 shows the comparison of the moments $\Delta_{11}, \Delta_{12}, \Delta_{13}, \Delta_{14}$, and Δ_{22} predicted from the theory versus the same quantities obtained from simulations. The agreement is good.

6.2 Single Particle Dynamics with Noise

In Section 4 we distinguished the motion of one particle in two contributions: the unperturbed motion plus a stochastic term. When we include the stochastic terms $\Delta x_k[\mathbf{N}]$, the motion become $x_k(s) = \hat{x}_k(s) + \Delta x_k[\mathbf{N}](s)$. Due to the random nature of the noise we expect the average position of the beam be $\langle x_k(s) \rangle_{\mathbf{N}} = \hat{x}_k(s)$. The spread form this value is measured by the variance

$$\langle (x_k(s) - \hat{x}_k(s))^2 \rangle_{\mathbf{N}} = \langle \Delta x_k^2 \rangle_{\mathbf{N}} = \Delta_{kk}$$

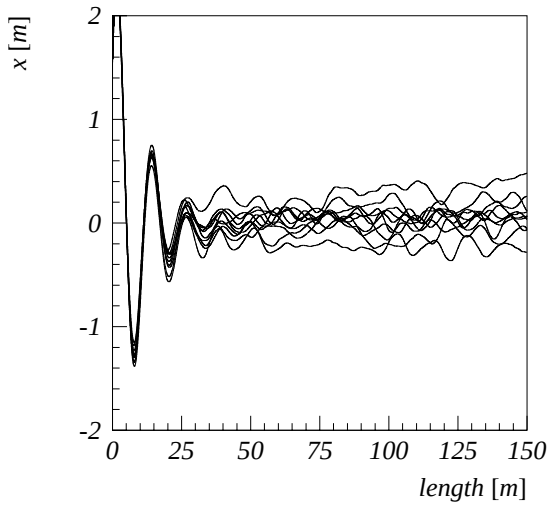

Figure 5: Effect of the diffusion over 10 repetition of the tracking of one particle in a uniform solenoidal cooling channel.

Most of the possible positions of the particle, at the longitudinal position s, are bounded within 3 standard deviation (99.7%) that is

$$|x_k(s) - \hat{x}_k(s)| < 3\sqrt{\Delta_{kk}}$$

Since the description of the cooling process for one particle is simplified by looking at the radius of the particle R and the normalized transverse kinetic energy E_k, we give next the effect of the noise on the evolution of R, E_k. With direct overestimates it is possible prove that (see appendix A)

$$R(s) \leq \hat{R}(s) + 3\sqrt{2}\sqrt{\Delta_{11}(s)} \tag{33}$$

and

$$\sqrt{E_k(s)} \leq \sqrt{\hat{E}_k(s)} + 3\sqrt{\Delta_{22}(s)} \tag{34}$$

We checked Eq. 33: Fig. 7 shows that the composition of the theoretical dump (red curve) with the theoretical noise (blue curve) bound one particle's trajectory and Fig. 8 shows that this result holds repeating 10 times the same simulation.

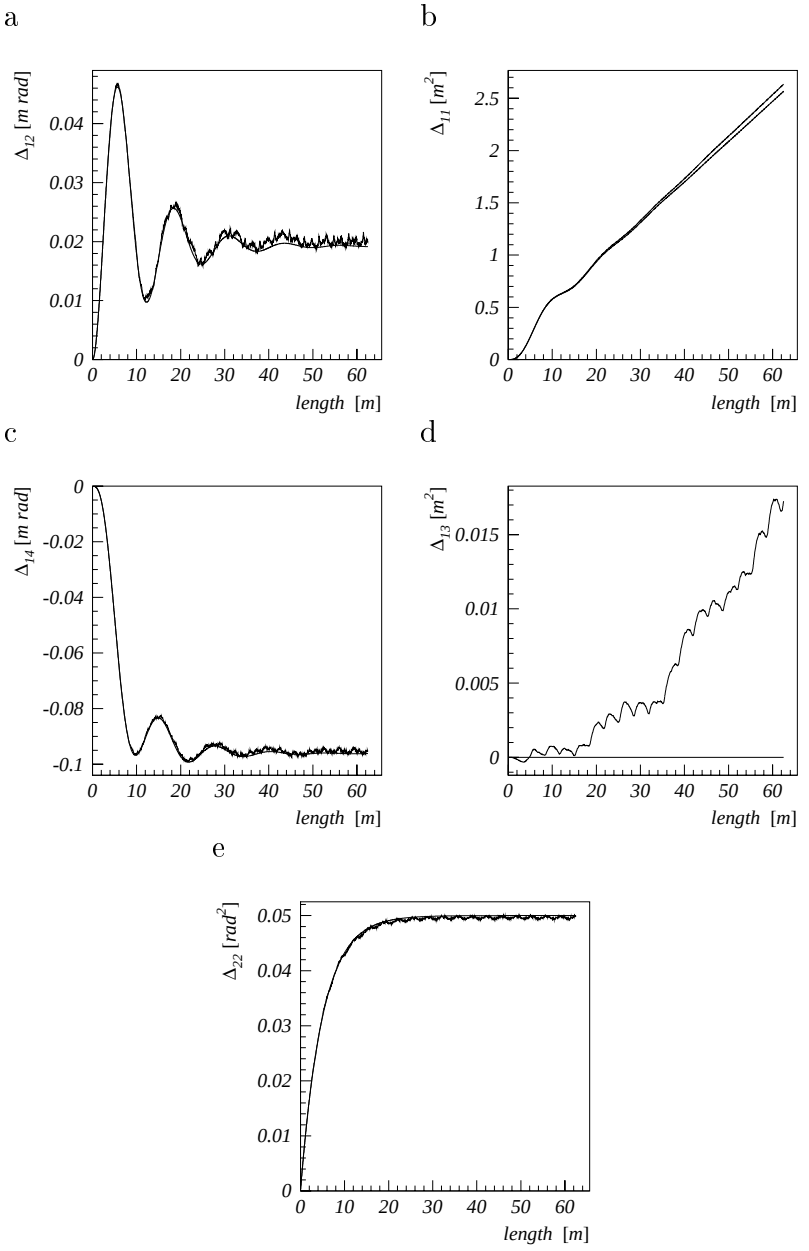

Figure 6: Comparison of the theoretical second order moments with simulation results obtained repeating 20000 the particle's tracking.

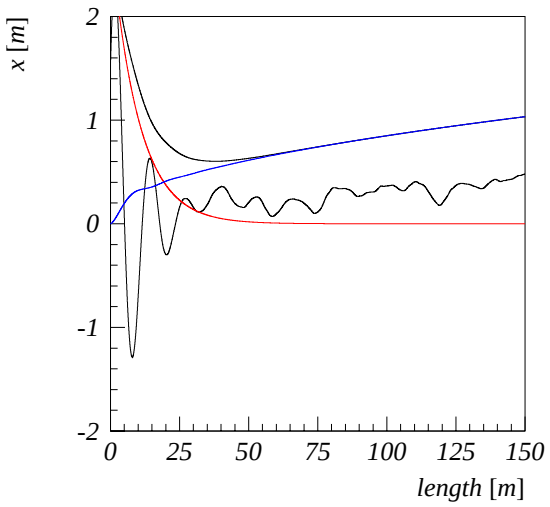

Figure 7: Example of how the composition of the theoretical dump (red curve) with the theoretical noise (blue curve) bounds a particle's trajectory

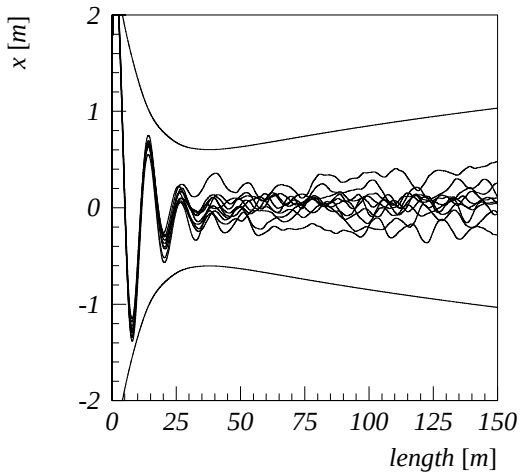

Figure 8: Comparison of the theoretical envelope versus 10 curves obtained in the uniform solenoidal cooling channel. The picture shows that the theoretical prediction bounds practically all the possible trajectories.

Substituting the expression for $\hat{R}(s), \Delta_{11}(s), \hat{E}_k(s), \Delta_{22}(s)$ we find

$$R_{max} = R_0 e^{-ds} + 3\sqrt{\frac{\alpha}{d(k^2+d^2)}}\sqrt{1 - e^{-2ds} + 2ds} \tag{35}$$

and

$$\sqrt{E_{max}} = \sqrt{E_{k0}} e^{-ds} + 3\sqrt{\frac{\alpha}{2d}(1 - e^{-2ds})} \tag{36}$$

Eq. 35, and Eq. 36 can be rewritten in term of the parameter

$$\chi = \frac{R_0}{3}\sqrt{\frac{d(k^2+d^2)}{\alpha}} = \frac{1}{3}\sqrt{\frac{2E_k d}{\alpha}}$$

and defining the normalized radius $\mathcal{R} = R_{max}/R_0$ and the rescaled transverse kinetic energy $\mathcal{E} = E_k/E_{k0}$ we find

$$\mathcal{R} = \sqrt{e^{-2ds}} + \frac{1}{\chi}\sqrt{1 - e^{-2ds} + 2ds} \tag{37}$$

$$\mathcal{E} = \left(\sqrt{e^{-2ds}} + \frac{1}{\chi}\sqrt{1 - e^{-2ds}}\right)^2 \tag{38}$$

In Fig. 9 we benchmarked Eq. 37, and Eq. 38. We computed from simulations R_{max}, and E_k over 10000 repetition starting from the same initial condition. In both pictures a), and b) we plot the max R and the max E_k at each integration step and the correspondent theoretical curves. The agreement is good.

Equation Eq. 37 shows the evolution of the normalized particle's radius. Once χ is fixed the radius is function of $2ds$ and $\mathcal{R}$ exhibits two regimes according to the value of χ. If $\chi < 2.55$, $\mathcal{R} \geq 1$ growths with s (Fig. 10b,c dashed line). Physically this means that at $s = 0$ the random transverse shifts induced by the absorber are already comparable with R_0: the particle is in a diffusive dominated regime. If R_0 is bigger enough ($\chi > 2.55$), the random noise produces a small effect on the dumping of R. However the dumping will go on until R become again comparable with the absorber shifts (at the longitudinal position s_R) and afterward the diffusive regime start again (see

a b

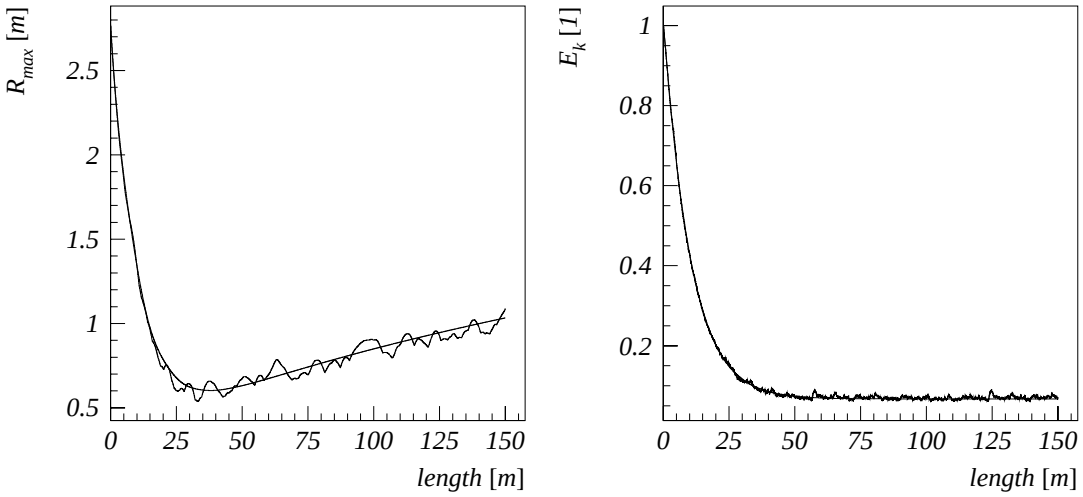

Figure 9: In a) we compare the envelope of $\sqrt{x^2+y^2}$ over 10000 repetition of the integration from the same initial condition. The continuous line represents the theoretical solution. In b) we consider the envelope of E_k for the same simulation, again the continuous line represents the theoretical prediction.

Fig. 10a dashed line). The transition can be equivalently expressed in terms of a kinetic transition energy as $E_{k,t} = 29.26\,\alpha/d$. A reduction of the initial kinetic energy E_{k0} will reduce the transition position s_R. When $s_R = 0$ the dumping regime disappears and only the diffusive regime will remain (form Fig. 10a to Fig. 10b dashed line).

To the rescaled transverse kinetic energy $\mathcal{E}$ (Eq. 38), a similar interpretation applies. If $\chi > 1$ the kinetic energy is bigger then the absorber noise and the cooling channel takes energy and reduces the transverse kinetic energy until a stationary state is reached (Fig. 10a,b solid line). If $\chi < 1$ the particle's kinetic energy is smaller than the average induced by the absorber and consequently E_k will increase reaching the equilibrium kinetic energy $E_{k,e} = 1/\chi^2$ (Fig. 10c solid line). Note that $\mathcal{E}$ reaches the local maximum of $\mathcal{E} = 1 + 1/\chi^2$. This means that even when the kinetic energy is dumped,

a b c

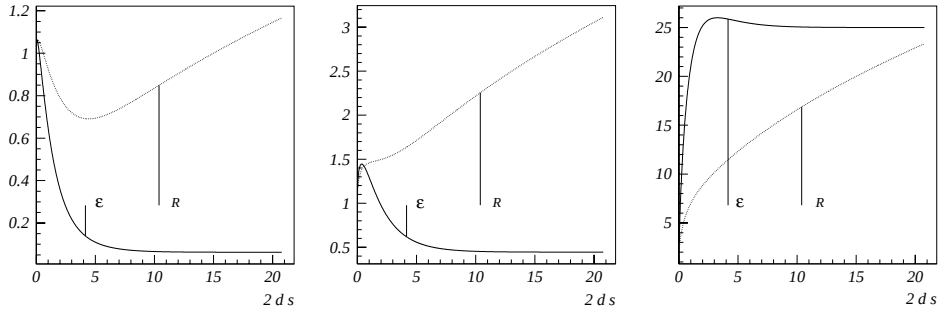

Figure 10: Evolution of $\mathcal{E}$ and $\mathcal{R}$ as function of $2\,d\,s$ for 3 different energies: a) $\chi = 4$, b) $\chi = 1.5$, c) $\chi = 0.2$

in some point, the contribution of the noise may cause an increase of the total kinetic energy. This local E_k growths is big when the contribution of the particle kinetic energy and of the heating are of the same order ($\chi \sim 1$). Note also that the transition of regime for $\mathcal{R}$, and $\mathcal{E}$ does not happen at the same energy! This is because the noise does act directly on the transverse momentums and with an integrated effect on the positions.

It is useful to find at what length $\mathcal{R}$ reaches its minimum (only when $\mathcal{R} < 1$). Once fixed χ we can find where $\mathcal{R}$ is minimum, i.e. $2ds_R$ and in the same longitudinal position compute the cooling factor $\mathcal{E}$. These results are shown in Fig. 11. From this picture we see that if χ is below a threshold $\chi_t = 2.55$ there is no optimum length because the absorber noise causes an heating from the beginning and $\mathcal{R}$ is never less than 1.

6.3 Single Particle Emittance and Beam Emittance

The 4D rescaled emittance of one matched particle $\epsilon_n(s) = \epsilon(s)/\epsilon_0$ is given the product $\mathcal{R}^2\mathcal{E}$. For ϵ_n, a picture similar to Fig. 11 can be built. Fig. 12 shows the optimum cooling length to minimize the single particle emittance. This picture is a fast tool to decide what energy matches (optimize) a certain cooling channel, or how long a cooling channel must be in order to reach the better cooling. If we consider a 'transverse monochromatic' beam, i.e. a beam with particles all having the same transverse kinetic energy, we can apply the single particle description to find the optimum cooling length for

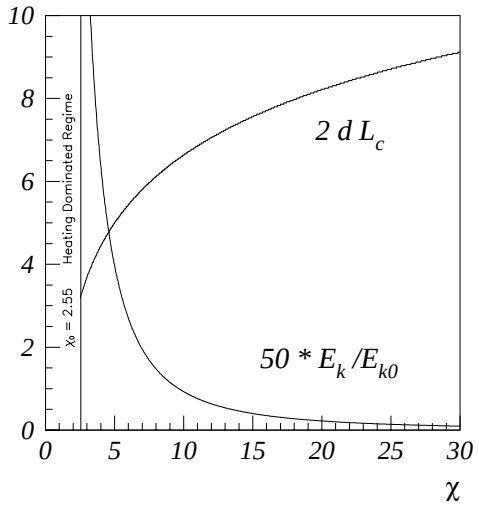

Figure 11: The upper curve shows the optimum cooling channel length in terms of $2dL_c$ as function of χ to minimize $\mathcal{R}$. The lower curve shows the cooling factor $50 * E_k/E_{k0}$ versus χ.

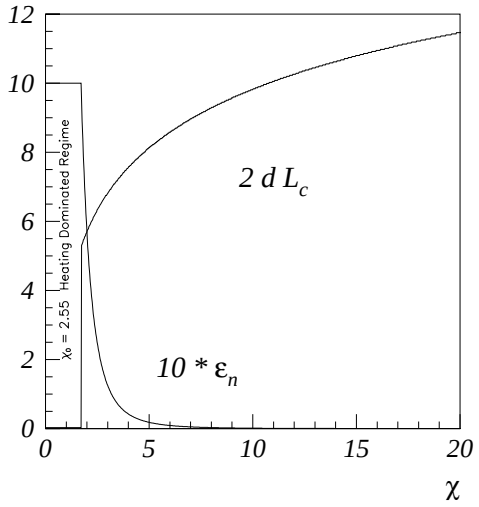

Figure 12: The upper curve shows the optimum cooling channel length in terms of $2dL_c$ as function of χ to minimize ϵ_n. The lower curve shows the cooling factor $10 * \epsilon_n$ versus χ.

the channel. If we do not consider the absorber noise, for every slice of the beam there is a limit x-y beam distribution of sizes $\Delta x_c, \Delta y_c$ in a very long cooling channel. This is because each particle's transverse kinetic energy gets dumped and particles fall into their guide rays transverse coordinates x_c, y_c. For an axisymmetric beam $\Delta x_c = \Delta y_c = R_l$ and the beam size can be written as $R(s) = R_l + R_0\mathcal{R}$. Since the maximum transverse kinetic energy of the beam is given by the same quantity for one particle i.e. E_k, the 4D rescaled emittance of the beam $\epsilon_{n,b}$ can be written as

$$\epsilon_{n,b}(s) = \left(\frac{1+\chi_b\mathcal{R}}{1+\chi_b}\right)^2 \mathcal{E}$$

where $\chi_b = R_0/R_l$. If the beam initially fills the solenoidal channel which has a radius R_s, then $\chi_b = R_0/(R_s - R_0)$. We see that the beam emittance evolution depends now from the two factors χ, and χ_b. In Fig. 13 we show for curves of constant χ_b the optimized length L_c as function of χ. In this picture we see the effect of the limit beam radius on the optimum cooling length: if $\chi_b << 1$ the beam size is big with respect to R_0 and we can propagate the beam through a longer cooling channel before the diffusive effect become relevant for the beam size. That's why in Fig. 13 there is a shift upward of the $2\,d\,L_c$ curves for small χ_b. On the other hand, for big cooling lengths the dump in E_k is almost complete and we find that all $\epsilon_{n,b}$ overlaps.

7 Validation Test with PATH [8] and Discussion

7.1 Test on the Cooling Strength

In order to better validate this theoretical model we considered one of the cooling cell of the 44 MHz section of the CERN ionization cooling scenario [8]. To test if the cooling is described correctly we removed all the solenoidal fields letting in the cell only absorber and RF cavities. We considered a design particle with kinetic energy of 200 MeV, which correspond for muons to an energy $E_0 = 305$ MeV, and $\beta = 0.938$. The 4 cavities of 2 MV have been merged in a single cavity of 8 MV and the phase in each cavity was taken zero (automatically set by PATH to maximize the acceleration). The

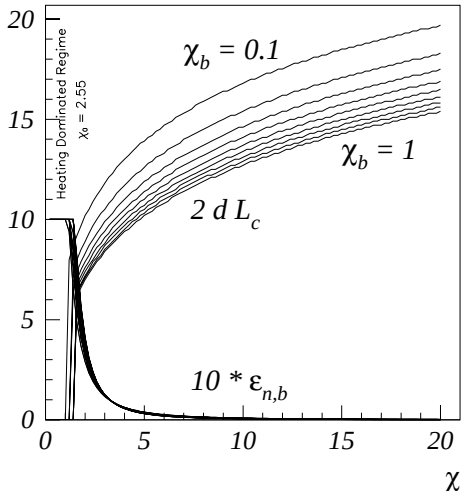

Figure 13: The upper curves show the optimum cooling channel length once fixed χ_b in terms of $2dL_c$ as function of χ. For this length $\epsilon_{n,b}$ is minimized. The lower curves show the cooling factor $10 * \epsilon_{n,b}$ versus χ for the correspondent χ_b

0.27 m length of the liquid hydrogen absorber was chosen such as to absorb 8 MeV so to let the design particle's energy unchanged at the exit of the cell. The test cell has so the length $L = 0.27$ m. The theoretical model developed in Sect. 6 predicts that for this test cooling cell a particle with an initial x'_0 at the entrance of the cell would be found at the exit with the reduced divergence according to

$$\Delta x'_{th} = -d\, L x'_0$$

where here $d = (\Delta E_0/E_0)/(L\beta^2) = 0.11$ m^{-1}. We tested this prediction by creating a pencil beam at a given initial angular position x' and computing the divergence at the exit of the cooling cell. The test was repeated for different initial angles. The next table reports these results.

x' mrad	Δ_{PATH} mrad	Δ_{th} mrad	error %
20	0.577	0.596	3.2
100	2.89	2.98	3.1
300	8.7	8.94	2.7
500	14.5	14.9	2.7
1000	28.9	29.8	3.0

We performed also a test on the dumping of the transverse normalized kinetic energy. We considered in this test the same cooling cell and pencil beam with an initial $x' = 0.2$ rad, $x = y = y' = 0$, and tracked it through 3 cells. We measure at the exit of each cell the quantity $\sqrt{E_k} = \sqrt{x'^2 + y'^2}$ and compare it with the theory which predicts a dump according to

$$\sqrt{E_k}_{out} = \sqrt{E_k}_{in} - d\, L \sqrt{E_k}_{in}$$

The next table summarizes these results

	$\sqrt{E_k}_{in}$	$\sqrt{E_k}_1$	$\sqrt{E_k}_2$	$\sqrt{E_k}_3$
PATH	0.2	0.1941	0.188	0.1824
theory	0.2	0.19404	0.18808	0.18212

we find errors between theory and multiparticle simulations less than 1 %.

7.2 Effect of the Noise on the Dynamics in a Test Cooling Cell

We also tested the effect of the noise on the particle dynamics. For the previous test cell we find from PATH $\alpha = 0.000215$ rad^2/m. A pencil beam

centered in $x = y = 0$ m, $x' = y' = 0.05$ rad was tracked with PATH through 100 cells. Each 10 cells from the particle's distribution we computed the quantities $\langle x \rangle$, $\langle x' \rangle$, $\langle xx' \rangle$, σ_x^2, $\sigma_{x'}^2$. The averages $\langle x \rangle$, $\langle x' \rangle$, are not effected by the absorber noise and evolve as a particle with initial coordinate $x = y = 0$ m, $x' = y' = 0.05$ rad in a cell without absorber noise but with transverse energy dump. In this case the equation of motion becomes $x'' + dx' = 0$ and the solution in the horizontal plane for the initial condition $x = 0$ m is

$$x = \frac{x_0'}{d}(1 - e^{-ds}) \quad x' = x_0' e^{-ds} \tag{39}$$

with x_0' initial horizontal angle of the tilted beam. The same solution holds in the vertical plane. In Fig. 14a,b we plot respectively these theoretical solutions for x, x' and the averages $\langle x \rangle$, $\langle x' \rangle$ from PATH. The growths of $\langle x \rangle$ is due to the lack of a focusing in the cooling cell. In fact we start with an initial transverse velocity $x' = y' = 0.05$ rad which is dumped by the cooling to zero, so the position $\langle x \rangle$ of the beam center increases reaching the asymptotic transverse position x_0'/d corresponding to the complete dump of the transverse kinetic energy. Fig. 14b shows the exponential dumping of $\langle x' \rangle$. The agreement between Eqs. 39 and simulations is good. Since the evolution of a single particle is given by $x_k = \hat{x}_k + \Delta x_k$, where $\hat{x}_k$ is the unperturbed solution given by Eq. 39, we can also predict the theoretical evolution of $\langle xx' \rangle$, σ_x^2, $\sigma_{x'}^2$. By using Eqs. 31 with $k = 0$ and Eqs. 39 we find

$$\begin{array}{l} \langle xx' \rangle = \frac{\alpha}{2d^2}\left(1 - e^{-ds}\right)^2 + \frac{(x_0')^2}{d} e^{-ds}(1 - e^{-ds}) \\ \sigma_x^2 = \frac{\alpha}{2d^3}\left(-3 - e^{-2ds} + 4e^{-ds} + 2ds\right) \\ \sigma_{x'}^2 = \frac{\alpha}{2d}(1 - e^{-2ds}) \end{array} \tag{40}$$

these functions are plotted in Figs. 14c,d,e with continuous lines respectively while with red spots are plotted the respective quantities obtained from PATH. The agreement is good.

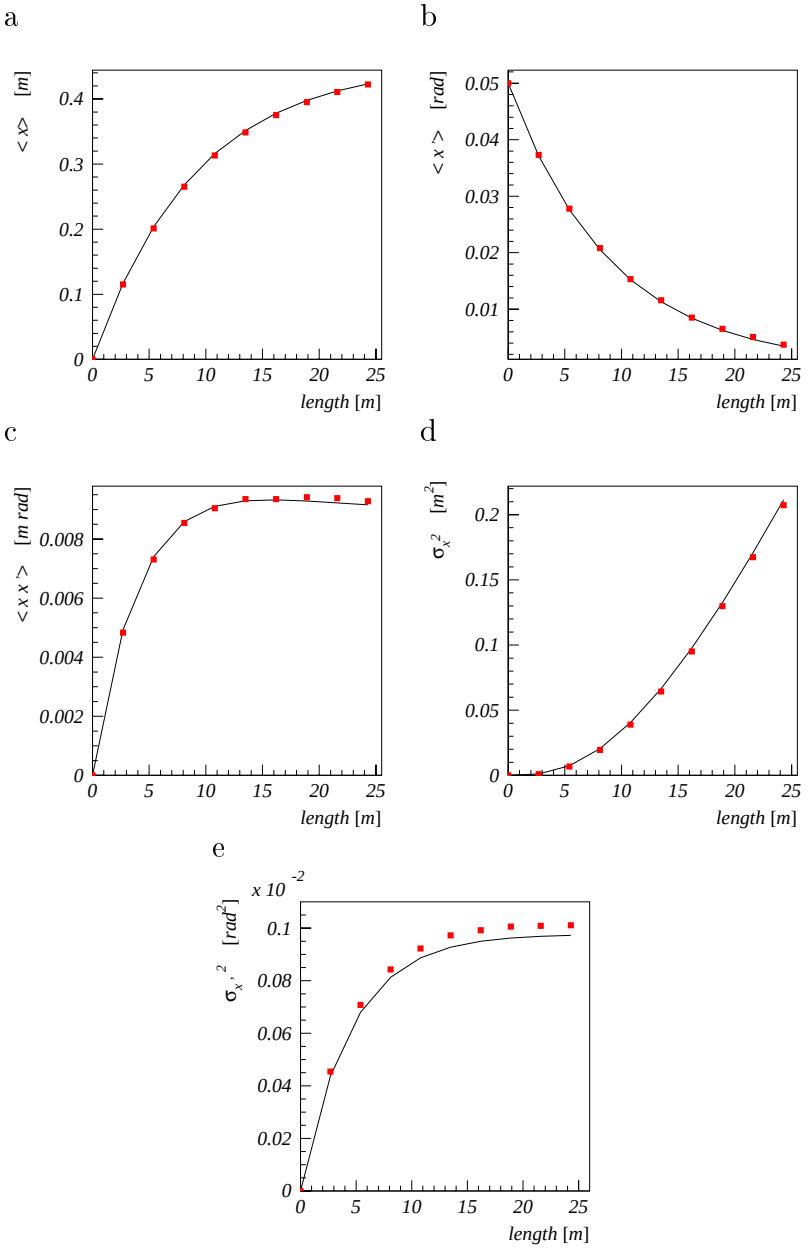

Figure 14: Comparison of the theoretical moments a) $\langle x \rangle$, b) $\langle x' \rangle$, c) $\langle xx' \rangle$, d) σ_x^2, e) $\sigma_{x'}^2$, with those obtained from PATH (dots).

7.3 Test on the Effect of the Noise on the Dynamics in a Uniform Cooling Cell

We consider here a benchmark between theory and simulations when the requirements of the theory are not completely fulfilled. We have considered the cooling cell of the 44 MHz CERN scenario where we have substituted the real solenoid with uniform solenoidal field (no fringe field). In order to keep the condition of thin absorber we reduced the absorber length to 0.0027 m however keeping artificially the energyloss we got with a length of 0.27 m. The benchmark of the position of the guiding ray obtained as the convergence point of the dumped motion resulted correct. In order to simplify the noise benchmark we considered a pencil beam with initial position $x = x' = y = y' = 0$. Fig. 15 shows the results from PATH compared with the prediction form the theoretical model. There is a still a good agreement for the the moments $\langle x^2 \rangle, \langle x'^2 \rangle, \langle xy' \rangle$. The reason is that the noise introduced by the absorber is 100 times smaller than a 0.27 m absorber length so the global dynamics still resemble the continuous. When we consider the same cooling cell but with a thick absorber (i.e. 0.27 m of absorber), we find first that the convergence of one particle to its guiding ray changes as well as the position of the guiding ray. For this reason, in order to avoid to recalculate the unperturbed motion, we considered the pencil beam placed in $x = y = x' = y' = 0$. Fig. 16 show these results. The global effect of the finite length of the absorber is to change the effective solenoidal strength of the cell: if we increase the solenoid strength of 25%, the curves theoretical curves $\langle x^2 \rangle, \langle x'^2 \rangle, \langle xy' \rangle$ would overlap with their correspondents theoretical curves.

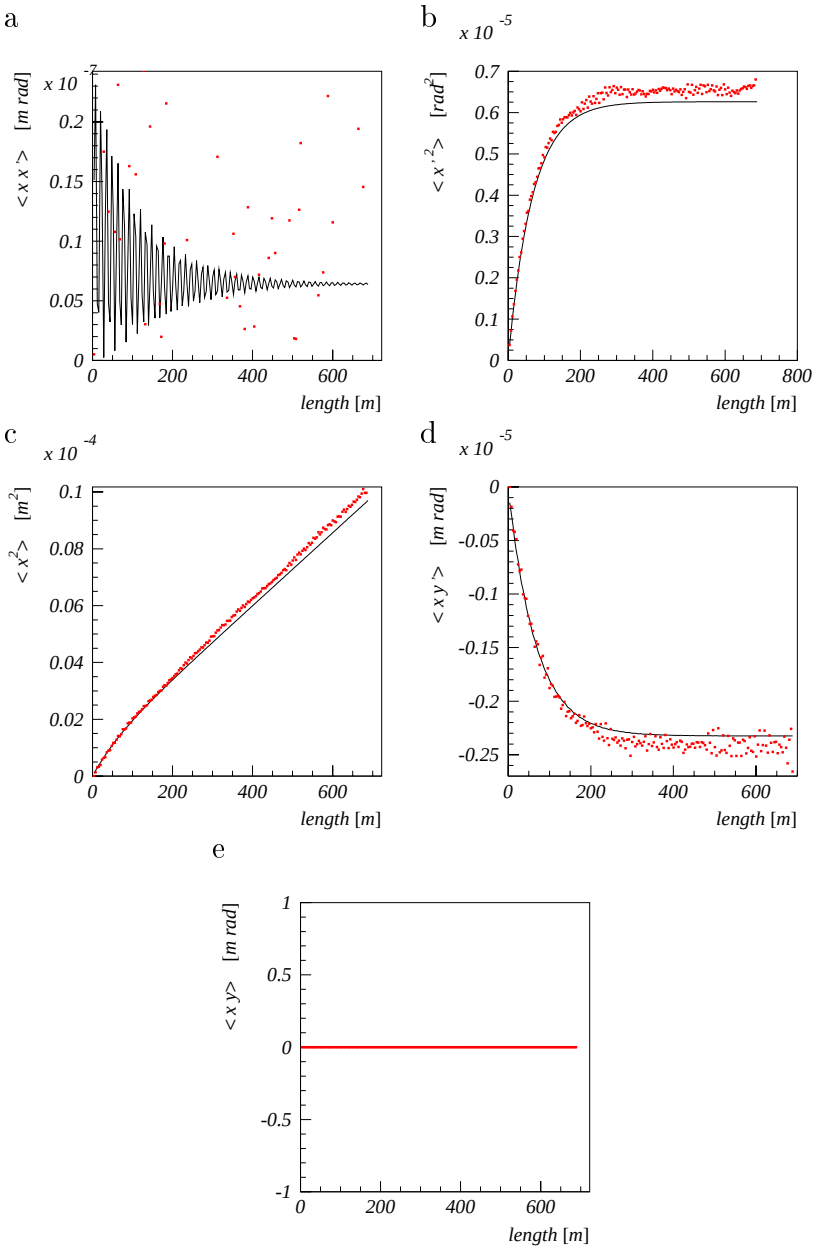

Figure 15: Uniform solenoidal filed with thin absorber. Comparison of the theoretical moments a) $\langle xx' \rangle$, b) $\langle x'^2 \rangle$, c) $\langle x^2 \rangle$, d) $\langle xy' \rangle$, e) $\langle xy \rangle$, with those obtained from PATH (dots).

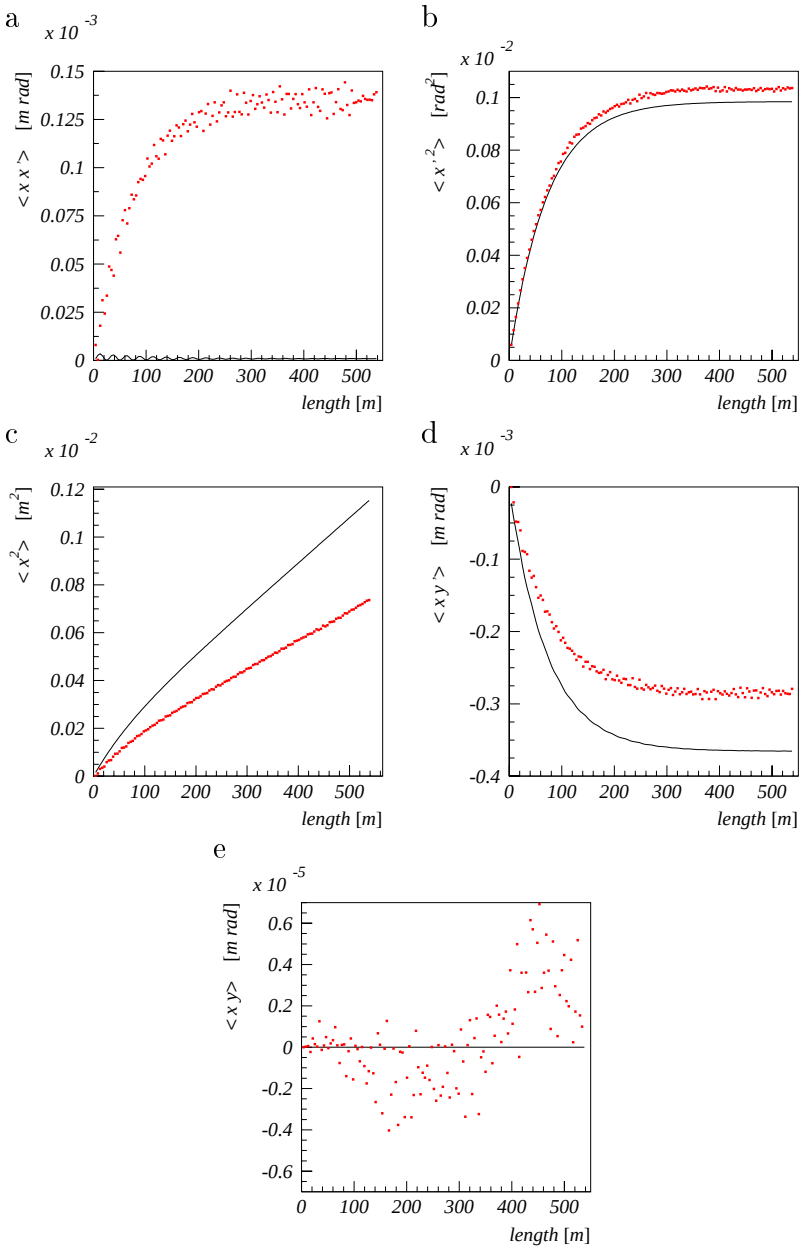

Figure 16: Cooling cell with uniform solenoidal field and thick absorber. Comparison of the theoretical moments a) $\langle xx' \rangle$, b) $\langle x'^2 \rangle$, c) $\langle x^2 \rangle$, d) $\langle xy' \rangle$, e) $\langle xy \rangle$, with those obtained from PATH (dots).

7.4 Test on the Effect of the Noise on the Dynamics in a Cooling Cell with Real Solenoids

We consider here a benchmark between theory and simulations when in the standard cooling cell (44 MHz CERN scenario) we use the realistic solenoid (hard edge fringe field). The cell has a liquid hydrogen absorber long 0.27 m. Since the effect of the fringe field on the single particle dynamics (in the edge approximation) is to give to give a transverse kick, we expect that the transverse energy dump will not follow the formula $E_k = E_{k,0}\exp(-ds)$ In order to simplify the noise benchmark we considered a pencil beam with initial position $x = x' = y = y' = 0$ Fig. 17 shows the result from PATH compared with the prediction form the theoretical description. The results from PATH show that $\langle x^2 \rangle$ noise does not growth linearly, but approach an asymptotic value. This stems from the fringe fields which transform the cooling cell more close to the uniform quadrupolar cooling channel described in Sect. 5. Fig 18 shows the prediction obtained considering the quadrupolar model.

8 Conclusion

We presented an uniform model of the ionization cooling an computed analytically the effect of the noise on the single particle dynamics. We studied two models: the uniform quadrupolar cooling and the uniform solenoidal cooling channel. For these two models we computed the effect of the absorbers noise on the single particle's dynamics and gave some predictions on the evolution of the emittance through the continuum cells. Finally we benchmarked the theoretical prediction with PATH cross checking theory and computer programs.

9 Appendix A

In this section we will prove Eq. 33, and Eq. 34. We start with R. The effect of the noise on the evolution of x is

$$x(s) = \hat{x}(s) + \Delta x(s)$$

Since most of the possible contributions of the noise are bounded within

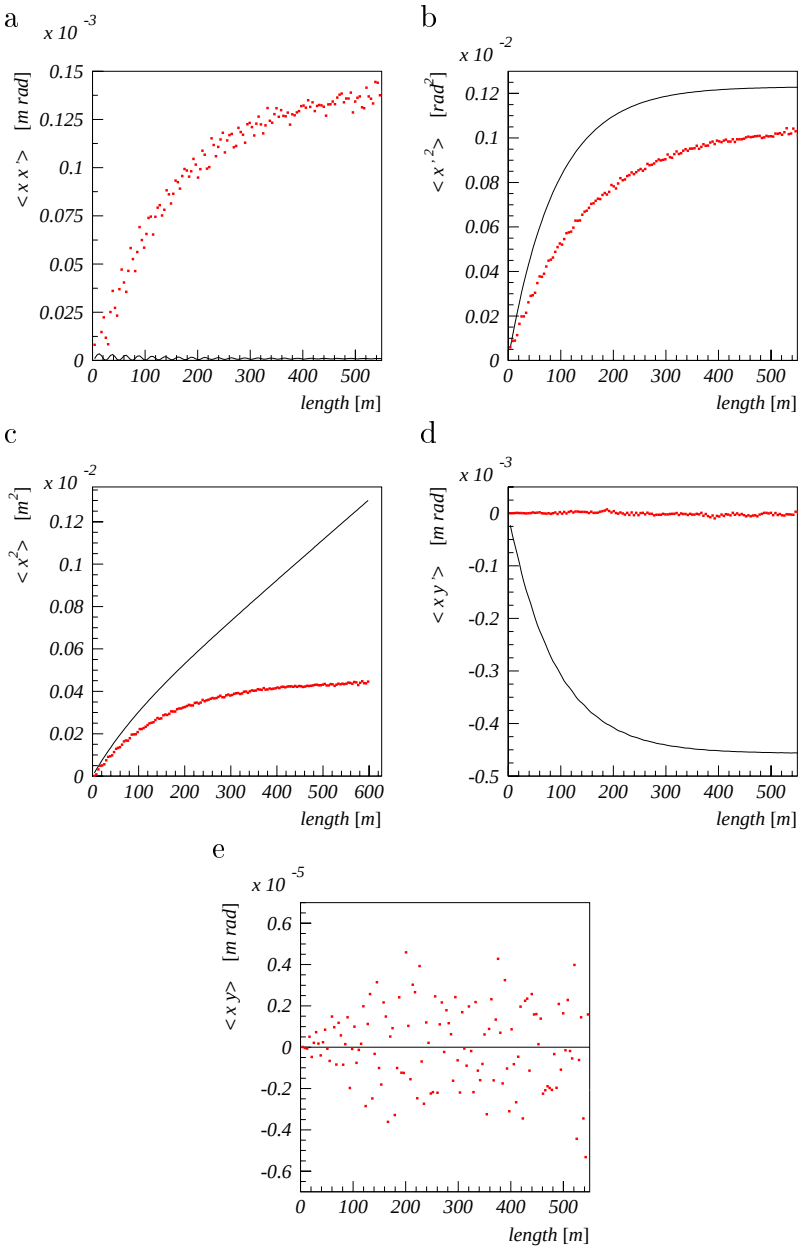

Figure 17: Cooling cell with realistic solenoids. Comparison of the theoretical moments a) $\langle xx' \rangle$, b) $\langle x'^2 \rangle$, c) $\langle x^2 \rangle$, d) $\langle xy' \rangle$, e) $\langle xy \rangle$, with those obtained from PATH (dots).

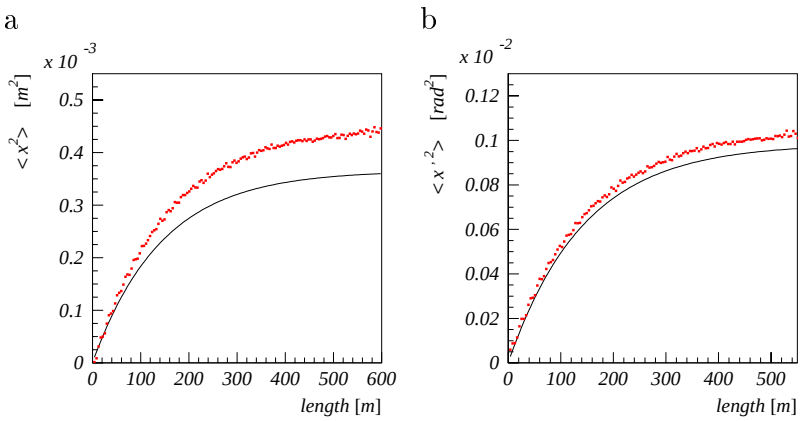

Figure 18: Cooling cell with realistic solenoids. Comparison of the theoretical moments a) $\langle x^2 \rangle$, b) $\langle x'^2 \rangle$, obtained from the quadrupolar uniform cooling model with those obtained from PATH (dots).

within 3 times the standard deviation we can write

$$x(s) = \hat{x}(s) + 3\phi_x(s)\sqrt{\Delta_{11}}$$

where $\phi(s)$ is a suitable number which is function of s. Note that $-1 < \phi_x(s) < 1$. The same argument applies for y. We conclude that at a certain longitudinal coordinate s the radius $R(s)$ is

$$R^2(s) = \hat{R}^2(s) + 9\Delta_{11}(\phi_x^2(s) + \phi_y^2(s)) + 2[\phi_x(s)\hat{x}(s) + \phi_y(s)\hat{y}(s)]3\sqrt{\Delta_{11}}$$

where we used the identity $\Delta_{11} = \Delta_{33}$. The constraint $x^2 + y^2 = \hat{R}$ allows to write

$$\phi_x(s)\hat{x}(s) + \phi_y(s)\hat{y}(s) \leq |\hat{x}(s)| + |\hat{y}(s)| \leq \sqrt{2}\hat{R}(s)$$

and since $\phi_x^2(s) + \phi_y^2(s) \leq 2$ we finally find

$$R(s) \leq \hat{R}(s) + 3\sqrt{2}\sqrt{\Delta_{11}}$$

Repeating the same argument one can prove Eq. 34.

10 Appendix B

A statistical description of the beam in a uniform cooling channel can include of the stochastic solution found in Section 4. At each longitudinal position,

the beam can be described by the the four-by-four sigma matrix defined as $\sigma_{ij}(s) = \overline{x_i(s)x_j(s)}$. We can decompose the motion of each particle as

$$x_i(s) = x_{c\,i} + x_{d\,i} + \Delta x_i$$

where: x_{ci} is coordinate of the guide ray; $x_{d\,i}$ is component of the motion that gets dumped by the cooling channel; Δx_i is the stochastic noise component. If we fix the noise $\mathbf{N}$ the sigma matrix become

$$\sigma_{ij}(s) = \overline{(x_{c\,i} + x_{d\,i} + \Delta x_i)(x_{c\,j} + x_{d\,j} + \Delta x_j)}$$

In order to remove the dependence on the noise, we average σ_{ij} over $\mathbf{N}$ and obtain

$$\sigma_{ij}(s) = \langle\overline{(x_{c\,i} + x_{d\,i} + \Delta x_i)(x_{c\,j} + x_{d\,j} + \Delta x_j)}\rangle_{\mathbf{N}}$$

that is

$$\sigma_{ij}(s) = \overline{(x_{c\,i} + x_{d\,i})(x_{c\,j} + x_{d\,j})} + \Delta_{ij}$$

Assuming that there are no correlations $\overline{x_{c\,i}x_{d\,j}}$, $\overline{x_{d\,i}x_{c\,j}}$ we finally find

$$\sigma_{ij}(s) = \overline{x_{c\,i}x_{c\,j}} + \overline{x_{d\,i}x_{d\,j}} + \Delta_{ij}$$

This result allows a direct calculation, in an average sense, of the beam rms emittance including the noise from the absorber.

11 Acknowledgments

I wish to thank prof. Giorgio Turchetti for the useful discussions and suggestions on stochastic equations.

References

[1] H. Haseroth, in *CERN Ideas and Plan for a Neutrino Factory*, edited by S. Chattopadhyay (Elsevier Scienc, NORTH-HOLLAND, 2000), p. 17, proceedings of the Nufact conference, Monterey CA, held March 29th - April 2nd.

[2] D. Neuffer, Part. Accel. **14**, 75 (1983).

[3] D. Neuffer, FERMILAB-Pub-96 140, Fermilab (unpublished).

[4] C. M. Ankenbrandt *et al.*, Phys. Rev. ST Accel. Beams **2**, 081001 (1999).

[5] K.-J. Kim and C. xi Wang, Phys. Rev. Lett. **85**, 760 (2000).

[6] G. Penn and J. S. Wurtele, Phys. Rev. Lett. **85**, 764 (2000).

[7] R. C. Fernow, in *ICOOL: a simulation code for ionization cooling of muon beams*, edited by A. Luccio and W. MacKay (IEEE, 445 Hoes Lane Piscataway, NJ 08854-4150, USA, 1999), Vol. 3, p. 3020, proceedings of the 1999 Particle Accelerator Conference, New York NY, held March 29th - April 2nd.

[8] A. Lombardi, CERN-NUFACT Note 34, CERN (unpublished).

[9] D. E. Gordon and S. R. Klein, The European Physical Journal C **15**, 163 (2000).

[10] G. Turchetti, in *Dinamica Classica dei Sistemi Fisici*, edited by Zanichelli (Zanichelli, Bologna, 1998), p. 584.

[11] C. W. Gardiner, in *Handbook of Stochastic Methods for Physics, Chemestry and Natural Sciences*, edited by Springer (Springer, Berlin, 1983), Vol. 13, p. 442.

[12] R. B. Palmer and R. Fernow, in *Beam Physics for Muon Colliders* (lectures given at the Accelerator School, Vanderbilt University, 1999).

[13] R. K. Cooper, Part. Accel. **7**, 41 (1975).